Vol. 47, No. 3 (2025) 426-442, DOI: 10.24874/ti.1911.02.25.05

Tribology in Industry

www.tribology.rs

RESEARCH

Effects of Recently Developed Severe Shot Peening Treatment on Mechanical and Tribological Properties of AISI 304 Steel

Khosro Shirvani[a,*], Behnam Salehnasab[b], Mohsen Mosleh[c], Raj Shah[d], Farshid Eyni[e], Behrang Asghari Shirvani[f]

[a]*Department of Mechanical Engineering Technology, Farmingdale State College, Farmingdale, NY, USA,*
[b]*Department of Mechanical Engineering, AU University, AL, USA,*
[c]*Department of Mechanical Engineering, Howard University, Washington, D.C, USA,*
[d]*Koehler Instrument Company, Holtsville, New York, NY 11742, USA,*
[e]*Germocore Company, Dusseldorf, Germany,*
[f]*Department of Mechanical Engineering, University of Ottawa, Ottawa, Canada.*

Keywords:

Shot peening
Residual stress
Wear
Tribology

* Corresponding author:

Khosro Shirvani
E-mail:
khosro.shirvani@farmingdale.edu

Received: 28 February 2025
Revised: 12 April 2025
Accepted: 19 May 2025

A B S T R A C T

This study investigates the effects of a newly developed gradient severe shot peening treatment (GSSP) on the mechanical properties and tribological behavior of AISI 304 steel. Some experimental tests, including microhardness and ball-on-disc wear tests, were conducted to evaluate the mechanical and tribological properties of both treated and untreated samples. The microstructure of the tested materials was analyzed using X-ray diffraction, optical microscopy, and scanning electron microscopy. Specimens treated with GSSP exhibited a reduction in mean crystallite size and an increase in hardness compared to specimens treated with conventional shot peening at a constant pressure. Samples treated by both conventional and gradient shot peening processes exhibited 50% to 75% of the wear experienced by non-treated steel specimens. An important finding of this study is that while the microhardness improvement in conventional shot pinning diminishes at a depth of 0.3 mm, it is sustained at depth of 0.4 mm and beyond in the GSSP. This study demonstrates the potential of the gradient severe shot peening technique to improve the mechanical properties of AISI 304 steel, primarily by reducing crystallite size and increasing hardness.

1. INTRODUCTION

To improve performance, reduce weight, and increase service life in mechanical components many mechanical treatments were invented and developed. For example in the energy sector, the improvements in materials and components used in gas turbine engines are a top priority for this industry [1]. Most damage mechanisms such as fatigue, fracture, and wear which can fail components create and initiate from the surface of components; therefore, surface treatments play an

important role in the service life of components [2–5]. Among failure mechanisms, wear is one of the most important and it is directly related to surface or exterior layers of materials [6–8]. Compressive residual stress and grain refinement directly affect material properties and are of importance in surface treatments [9]. The shot peening process is one of the severe plastic deformation methods and it can improve wear resistance by introducing compressive residual stress (CRS) in the depth of material under the surface and producing a higher microhardness [10,11]. The shot peening process makes permanent plastic deformation in the exterior layers of the component surface, which leads to structural changes, strain hardening, and compressive residual stress in the region. Based on the input energy level, the shot peening process can be classified into the conventional and severe shot peening processes [12]. During the shot peening process, many small metallic shots impact the surface, and resulting from each impact, surface layers undertake compressive plastic deformation, and a compressive residual stress field is generated. Among the different surface treatment techniques, severe shot peening (SP-S) is one of the common processes for industrial components and it is the conversion of conventional shot peening by increasing kinetic energy. The main benefit of SP-S is to reduce grain size to a nanoscale regime and induce a deep layer with high compressive residual stress [13,14]. AISI 304 steel alloy is one of the most widely used stainless steel in automotive and energy industries and has been widely investigated in terms of the effects of different surface mechanical attrition treatments (SMAT) on structural integrity and surface hardening [15–18]. However, some studies showed that AISI 304 stainless steel has low wear resistance in dry and wet sliding conditions and severe abrasive wear has been reported [19–23]. Some studies have been carried out to evaluate the effect of shot peening process parameters such as shot diameter [24–26], shot velocity [25], Almen intensity [27–29], and surface coverage [30,31]. Also, many researchers have studied the effect of the shot peening process on mechanical and metallurgical characteristics [28,32–34]. In addition, some studies have investigated the role of the shot peening process on the failure mechanisms such as fatigue behaviors [35–39], fretting wear properties [40–42], and corrosion performances [43–45]. There has been limited research examining the impact of different shot peening methods on tribological characteristics, as explored in this study. For instance, Silva et al. [7] investigated the effects of shot peening on residual stresses and tribological performance of cast and austempered ductile iron. The findings indicated that shot peening induced a transformation of retained austenite to martensite, resulting in increased hardness. However, this hardness enhancement was inadequate to offset the adverse effects of heightened surface roughness induced by shot peening on wear behavior. Kovaci et al. [46] delved into the impacts of shot peening pre-treatment and plasma nitriding parameters on the structural, mechanical, and tribological attributes of AISI 4140 low-alloy steel. The investigation revealed that the shot peening treatment resulted in the formation of finer grains, the induction of compressive residual stresses on the surface, and an augmentation in the diffusion kinetics of the samples. Moreover, surface hardness and residual stresses exhibited an upward trend with increasing shot peening density. Additionally, the combined application of shot peening and plasma nitriding treatments led to enhancements in the wear resistance of the material, with the highest level of wear resistance observed in the shot peened + plasma nitrided samples. Wei et al. [47] investigated the impact of wet shot peening (WSP) on the wear and corrosion behavior of AISI 304 stainless steel through dry reciprocating sliding wear tests. The findings from the tests revealed a notable enhancement in wear resistance due to WSP treatment. Interestingly, the wear mechanism observed in both as-received and wet shot peened AISI 304 stainless steel involved a combination of abrasive and adhesive wear. Gopi et al. [48] investigated the microstructure, friction, and wear properties of shot peened 316L stainless steel. The findings demonstrated that the shot peening process enhances the wear properties of the material. Yildiran Avcu et al. [49] investigated the surface, subsurface, and tribological characteristics of Ti6Al4V alloy subjected to shot peening under various parameters. The findings indicated that, following dry sliding wear tests, the mass loss of the peened samples (specifically S60 for 15 minutes) was 25% higher compared to the un-peened samples, albeit with a 12% decrease in the coefficient of friction. Notably, plastically deformed regions and micro-scratches were discernible on the worn surfaces, aligning predominantly with adhesive and abrasive wear mechanisms. Zhang et al. [50] delved into the tribological behavior and corrosion resistance of S30432 steel following various shot peening processes. The findings

indicated that, compared to the original S30432 steel, the wear resistance of all shot-peened samples improved under the measured loads. This enhancement was predominantly attributed to the elevated hardness of the gradient hardening layers. Trung et al. [51] investigated the impacts of shot peening pressure, media type, and double shot peening on the microstructure, mechanical, and tribological properties of low-alloy steel. The findings revealed that both shot peening pressure and media type exerted significant effects on the surface roughness, hardness, microstructure, wear resistance, and friction of the shot peened AISI 4340 steel samples.

Recently, Maleki et al. [52] introduced gradient severe shot peening (GSSP) as a novel shot peening process. Consequently, this study investigates the microstructures, residual stress, and mechanical and tribological properties of AISI 304 steel treated using this method. Notably, the influence of the GSSP process on the tribological properties of AISI 304 is examined for the first time. Experimental tests were conducted to scrutinize the microstructure, grain size, surface topography, microhardness, and residual stresses of each shot-peened specimen. The microstructure of the shot-peened specimens was evaluated utilizing optical microscopy and scanning electron microscopy, while mechanical properties were assessed via microhardness and roughness measurements. Residual stress was determined using the XRD method. Furthermore, the wear behavior was investigated through a pin-on-disc test, and the worn surface topology was examined using scanning electron microscopy (SEM). Finally, the various shot-peened specimens were compared based on the aforementioned measurements.

2. MATERIAL AND EXPERIMENTAL PROCEDURE

2.1 Materials and specimens

The austenitic stainless steels have an austenitic structure in the annealed condition. AISI 304 stainless steel with chemical composition of (0.027C, 0.35Si, 1.61Mn, 0.037P, 0.018S, 18.03Cr, 0.29Mo, 8.43Ni, 0.14C, and Bal. Fe in wt.%) is characterized by high corrosion resistance and high toughness; thus, it is broadly used in automotive, food, and power industries; therefore, it is nominated for experimental testing in this study. AISI 304 stainless steel specimens were interrupted from a sheet with 3 mm thickness by using an Electrical Discharge Machine (EDM) to the form of a rectangular cube with dimensions of 50×50×3 mm. Each of the specimens was separately prepared for each of the tests. The mechanical properties of the material are summarized in Table 1.

Table 1. Mechanical properties of the supplied material.

YS (MPa)	UTS (MPa)	Elongation (%)	Hardness (HRC)	YS (MPa)
550	750	40	28	550

2.2 Design of experiments for shot peening

The shot peening process was carried out according to the SAE AMS2430 standard [53]. The peening balls were made from SAE J2175 and the diameter and hardness of the balls are 0.5 mm and 60 Rockwell C, respectively. The shot peening was performed by using an air blast shot peening machine. All specimens are shown in Fig. 1. In GSSP, instead of employing a consistent projection pressure, we explore variant pressures. Here, we introduce two distinct GSSP methodologies: ascending severe shot peening (SP-A) and ascending-descending severe shot peening (SP-AD), each delineated based on pressure variation trends. As illustrated in Fig. 2, in SP-A, the projection pressure steadily increases, whereas in SP-AD, it gradually rises to a peak before declining.

The conventional shot peening treatment is converted to severe shot peening treatment by increasing surface coverage to 1500% [54]. The applied parameters of the shot peening process on the specimens are shown in Table 2. Four different types of shot peening treatments were utilized: conventional (SP-C), severe (SP-S), and two variations of GSSP methodologies; SP-A and SP-AD. Different shot peening processes are described in detail in reference [55]. Also, the peening duration in these processes is 15 times longer than SP-C, which was 10 seconds for 100% surface coverage. The SP-A and SP-AD processes mitigate the adverse effects of overshot peening (OSP) while retaining the advantageous outcomes of surface nano-crystallization, surface hardening, and the induction of compressive residual stresses (further elaborated in Ref. [52]). The corresponding pressure versus peening duration of the considered surface treatments is shown in Fig. 2.

Table 2. Shot peening process parameters.

Specimen ID	Pressure (Psi)	Almen Intensity (mmA)	Peening Duration (s)	Surface Coverage (%)
NSP	-	-	-	-
SP-C	55	0.3	10	100
SP-S	55	0.3	150	1500
SP-A	40 → 55	0.25 → 0.3	150	-
SP-AD	40 → 55 → 40	0.25 → 0.3 → 0.25	150	-

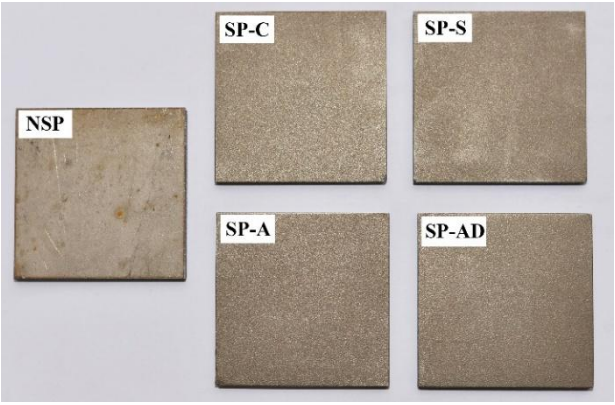

Fig. 1. Photographs of prepared flat specimens for testing: the NSP specimen is unprocessed, while SP-C, SP-S, SP-A, and SP-AD specimens have been treated with respective shot peening methods. Note the visual differences in surface appearance due to varying peening intensities and sequences.

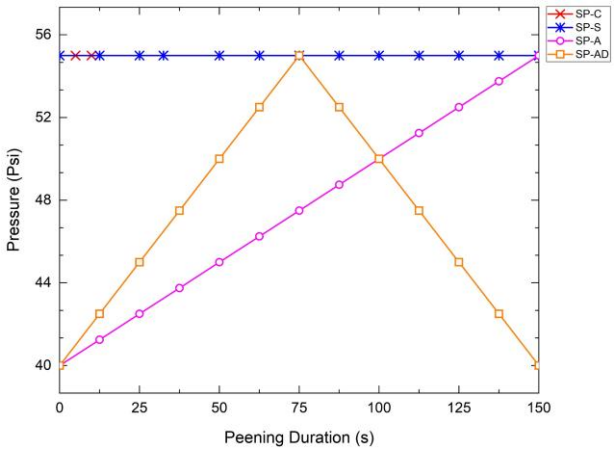

Fig. 2. Schematic diagram illustrating the pressure profiles applied during shot peening treatments. SP-A and SP-AD represent gradient severe shot peening (GSSP) processes.

2.3 Microstructure evaluation

Sample preparation was performed by following standard metallographic procedures and specimens were etched with 2% Nital solution. the OLYMPUS optical microscope was used to observe the cross-sectional microstructure characterization of different shot-peened specimens.

2.4 Residual stress measurement

The residual stress profile along the depth induced by the shot peening process was examined using the X-ray diffraction (XRD) method. Cu-Kα radiation at 40 kV, 30 mA, and 1°/min, and the X-ray beam spot size is about 1×1 mm was used in the XRD test method. To obtain the depth layers of the specimen material, measurement was performed step by step by removing a layer of material with 0.1mm through electrochemical machining (ECM) with a solution of acetic acid (94%) and perchloric acid (6%). The depth was accurately measured by using a micrometer, with a resolution of 0.01 mm.

2.5 Microhardness and surface roughness measurement

The surface roughness profile of the shot-peened specimens was evaluated by a digital roughness tester machine. A cut-off value of 0.8 mm and 2 mm were used for the non-shot peened and shot peened specimens, respectively. Three times measurements were carried out for each surface condition and the mean values were recorded. The roughness parameters are presented based on the ISO 4287 standard. To study the effect of the shot peening process on the microhardness of the specimens, depth-resolved Vickers microhardness measurements were carried out on cross-sections of the specimens using a microhardness test machine with a 10 gf load and a 10-second holding time, in accordance with ISO 6507. Surface roughness of the polished cross-sections used for hardness testing was also measured to ensure that preparation artifacts did not affect the microhardness results. The measured roughness values were below 0.05 μm (Ra), indicating that surface finish was sufficiently smooth for accurate microhardness assessment. Microhardness measurements were performed on the matrix of each specimen cross-section at depth intervals of 50 μm. At each analyzed depth, three independent indentations were made (n = 3), and the average

value was reported. The standard deviation for each data point was calculated and remained below 5%, confirming the reliability and consistency of the measurements.

2.6 Wear test procedure

Wear tests were carried out by using a sliding pin-on-disc in dry conditions with a conventional tribometer to evaluate the tribological behavior of the specimens under different shot peening conditions. To ensure duplicability of results, all wear tests were performed under the same environmental condition, i.e., at room temperature (25 °C) and a humidity of 25%. AISI 52100 steel pins of 9mm radius were used as their counterparts in the test. The hardness of AISI 52100 was 62-64 Rockwell C. The test specimen has a dimension of 20×20×4 mm. The applied load was 10N which created a Hertzian contact stress of 40.3 MPa. The rotational speed was 530 rpm which created a linear sliding speed of 0.5 m/s. The total sliding distance in each test was 1000 m. The tests were repeated once for each experimental condition. Wear volume was determined by separately weighing the mass of both the disc and the hard metal counterpart pin before and after testing each specimen. After each 100 m, the sample was taken out of the war machine, cleaned, and weighed. The wear mass was calculated by the difference between the initial and the subsequent weight of the test samples.

3. RESULTS AND DISCUSSIONS

3.1 Microstructural analysis of specimens

A series of optical microscopy and XRD analyses were carried out to evaluate the microstructures and grain sizes of the as-received and shot-peened specimens. The specimens were cut in the depth of the thickness with a wire-cut Electric Discharge Machine (EDM) and then the surface of the specimens was polished based on the metallographic process and etched for optical microscopy and image evaluations. Microstructural observations from the surface layer to depth for the as-received specimen and after shot peening treatments are shown in Fig. 3.

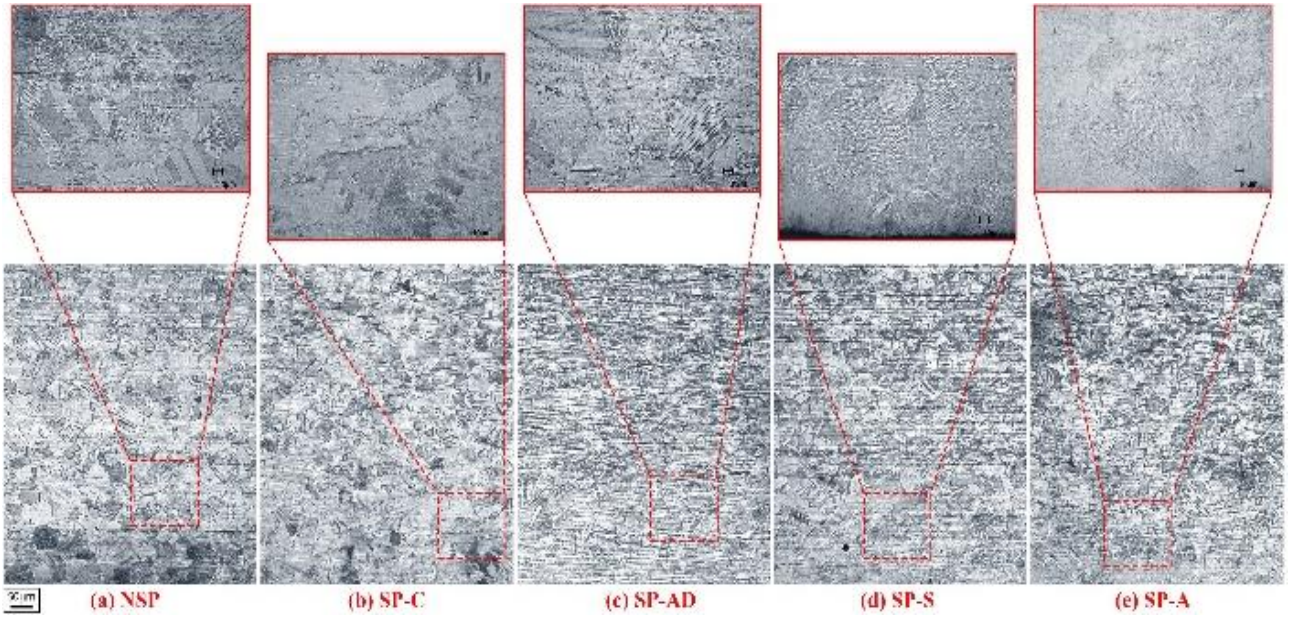

Fig. 3. Cross-sectional OM micrographs of the specimens.

It can be observed that the depth of the plastically deformed layers is increased by increasing the kinetic energy, and plastically deformed layers are enhanced; also, the grain refinement achieves by increasing the severity of shot peening treatment. As can be observed, the microstructures of all specimens are formed by austenite grains which inside them mechanical twining marks are observed; also, in the surface layer of the specimens slip lines are formed inside the grains due to cold work. As expected, the SP-C specimen has a less significant grain refinement due to lower kinetic energy. The mean grain size area was

measured using image analysis by using MIP® software for SP-C and NSP specimens as 42 and 26 μm2, respectively. Optical microscopy images and XRD grain size measurements show the most notable grain refinement was obtained for the SP-A followed by SP-S and SP-AD treatments. As can be seen, the grain's size reduced near the top surface layer. To evaluate the grain size of the shot-peened treated specimens at higher rates of kinetic energy, X-ray Diffraction (XRD) analysis is proposed [55]. Fig. 4 shows the XRD patterns of the specimens.

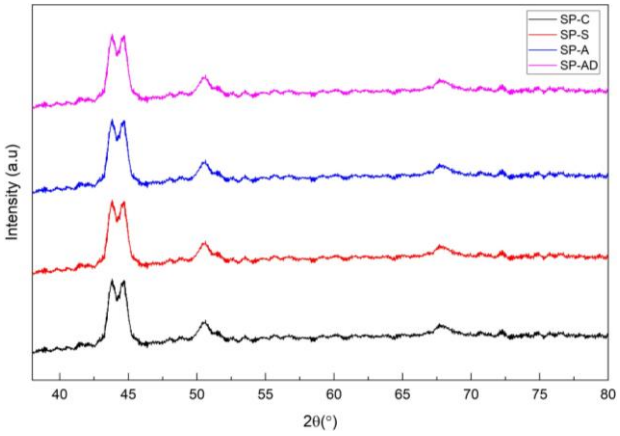

Fig. 4. XRD patterns of the specimens.

A general method for determining the mean crystallite size is used for determining the crystallite sizes of the specimens in the top surface layer. The full width at half maximum (FWHM) of a diffraction θ peak at Scherer's equation is given as [56]:

$$d_{XRD} = K\lambda / \beta \cos\theta \quad (1)$$

Where d is the crystal apparent size, θ is the diffraction angle, λ is the x-radiation wavelength, K is a constant close to unity, and β is the corrected FWHM. β can be obtained from the observed FWHM by convoluting the Gaussian profile modeling the specimen broadening βr, as follows:

$$\beta_r^2 = \beta_0^2 - \beta_i^2 \quad (2)$$

Where β_0 is the observed broadening and β_i is instrumental broadening. To determine the peak broadening with the crystallite size XRD method is used [57]. The results of the crystallite size of the specimens are presented in Table 3.

Table 3. Crystallite size of the specimens.

Specimen	NSP	SP-C	SP-S	SP-A	SP-AD
Crystallite size (nm)	42530	26215	81	79	85

There are many factors that can affect the XRD measurements such as microstresses, dislocations, and defects which were not considered in the determination of the size of the crystallite in this paper. Also, constants K and b_i and b_o were the default values for the typical XRD analysis. However, the XRD analysis was used as a comparative tool to access the crystallite size of non-treated, treated with conventional shot-pinning, and treated with severe shot peening samples. As Table 3 shows, there is reduction of over 99% in the crystallite size from conventionally shot-peened samples to the severe shot-peened samples.

3.2 Hardness and surface roughness measurement and analysis

Shot peening induces dimple-shaped deformations on the surface of treated specimens due to the impact of high-velocity shots, leading to increased surface roughness. To assess the effects of these impacts, both the surface roughness and microhardness of the treated specimens were measured. Microhardness measurements were particularly important for evaluating how plastic deformation affected the mechanical properties of the specimens. The variation in microhardness across the depth of the surface layer for the different specimens is illustrated in Fig. 5.

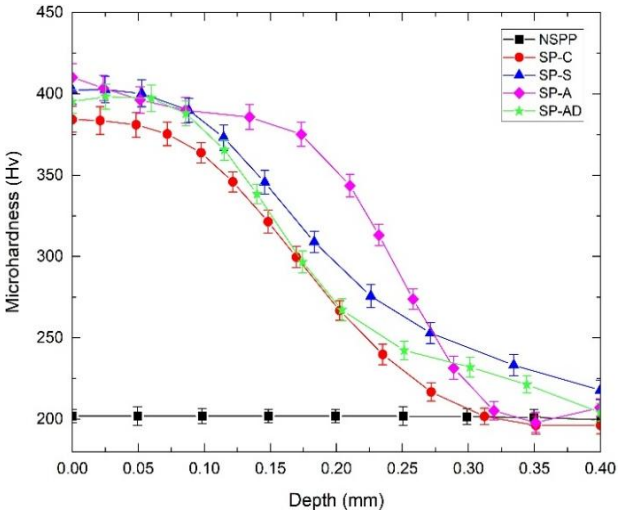

Fig. 5. Cross-sectional microhardness profiles of specimens.

These measurements showed a data scatter of less than 5%, ensuring reliable results. For non-shot-peened (NSP) samples, the microhardness remained consistent at 202.5 HV throughout the measurement depth. This stability reflects the lack of induced plastic deformation in these specimens. In contrast, shot-peened samples exhibited a decrease in microhardness as the measurement depth increased. The highest microhardness values were observed near the surface, where the effects of shot peening were most pronounced, with values gradually diminishing to a steady state of approximately 202.5 HV at a depth of 0.4 mm and beyond. This indicates that the plastic deformation and the associated hardening effects were limited to the surface and subsurface layers of the material. Among the shot-peened specimens, the lowest surface microhardness was observed in SP-C samples, with a value of approximately 370 HV. Conversely, SP-A samples showed the highest surface microhardness, measuring 410 HV. The enhanced hardness at the surface in SP-A samples suggests a more intense or effective peening treatment compared to the others. Notably, the SP-A samples retained higher hardness in the near-surface region, maintaining these elevated values up to a depth of 0.2 mm, indicating a more robust surface hardening effect compared to other treatments. Surface roughness (Ra and Rz) was measured for both shot-peened and non-shot-peened specimens using a Mitutoyo Surftest SJ-210 portable machine. Fig. 6 presents the surface roughness values and surface morphology for the different treatment conditions. The roughness measurements were taken as averages across three specimens for each test condition to ensure statistical relevance. The comparison between the treated and untreated samples clearly highlights the impact of different shot peening techniques on surface texture.

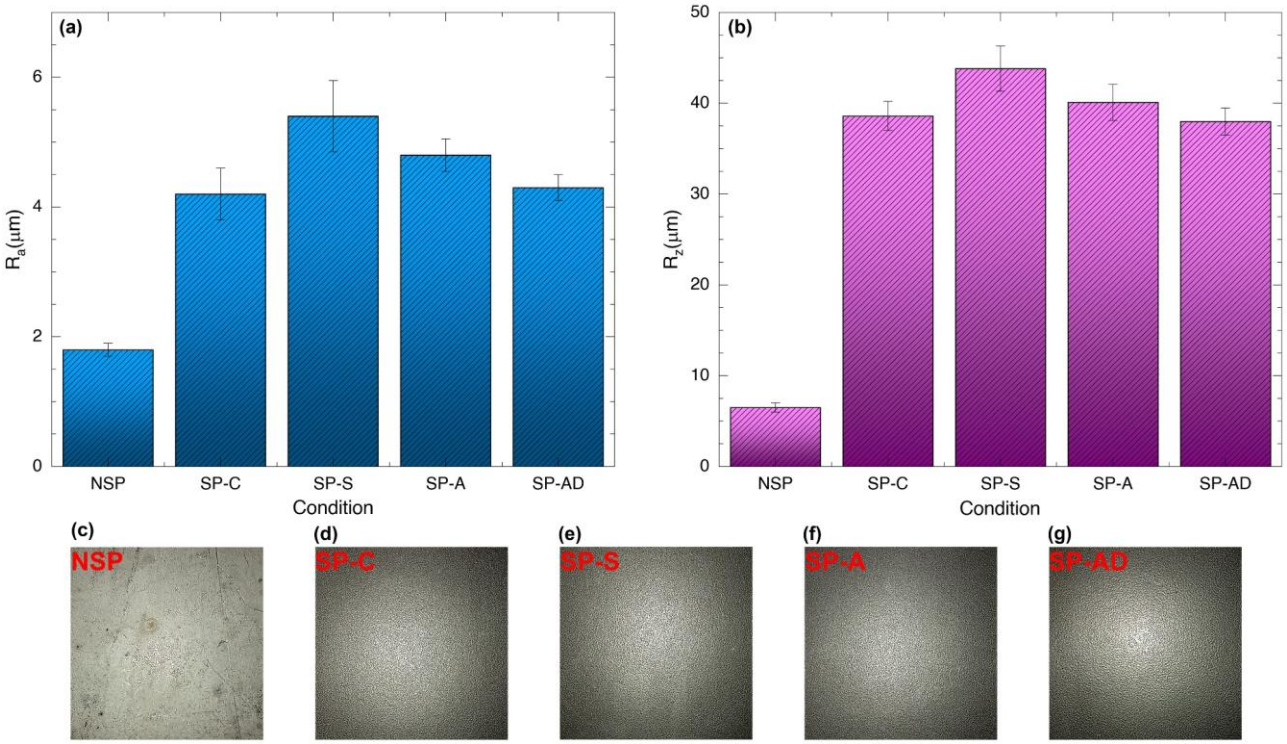

Fig. 6. Values of surface roughness in terms of R_a and R_z and surface morphology of specimens.

Among the treatment variations, gradient severe shot peening (GSSP) stood out as an innovative approach that involved gradually increasing the projection pressure during the process. Despite having the same exposure time as severe shot peening (SSP), GSSP's gradual pressure increase served as a pre-hardening step for subsequent higher-pressure peening. This gradual pressure application enhances the material's tolerance to shot impacts, resulting in less surface deformation and fewer defects. The controlled pressure ramp in GSSP ensures that the material experiences less aggressive surface damage, leading to a smoother finish. In contrast, conventional severe shot peening (SSP)

treatments apply a constant, high-impact pressure from the outset. This creates a rough surface with distinct dimple-shaped morphology due to the immediate and intense plastic deformation. However, when the pressure is applied in an ascending manner, as in the ascending severe shot peening treatment (SP-A), the surface becomes smoother, with lower roughness values. This is because the gradually increasing pressure mitigates the surface deformation, resulting in a more refined surface texture. Furthermore, the ascending-descending severe shot peening treatment (SP-AD) produced a surface with even smaller dimple-shaped morphologies and lower roughness compared to the SP-A treatment. In SP-AD, the initial ascending pressure phase induces plastic deformation, while the subsequent descending pressure phase acts as a re-peening process. This step effectively smooths the surface and reduces roughness, leading to improved surface morphology. The results demonstrate that gradient severe shot peening treatments, such as SP-A and SP-AD, yield smoother surfaces compared to conventional severe shot peening treatments. These methods successfully minimize surface defects and roughness while retaining the beneficial hardening effects induced by shot peening. While the R_z values shown in Fig. 6(b) appear similar across the shot peened specimens (SP-C, SP-S, SP-A, SP-AD), a closer examination of surface morphologies reveals important distinctions. The SP-A and SP-AD treatments produced more uniform and shallower dimples compared to the SP-S condition, which exhibited more irregular and pronounced surface indentations. Therefore, surface roughness values such as Ra and R_z should be interpreted in combination with SEM images to provide a complete understanding of the surface texture and its potential tribological implications. Although SEM images of surface defects are not presented in this study, the surface roughness measurements (Ra and Rz) and improved wear resistance suggest that GSSP-treated specimens (particularly SP-A and SP-AD) exhibit fewer and less severe surface defects compared to SP-S. This inference is consistent with prior literature [52], where the gradual pressure variation in GSSP is shown to mitigate surface damage while enhancing surface properties.

3.3. Residual stress analysis

Residual stresses in the films were assessed using the conventional X-ray diffraction (XRD) technique, carried out on a diffractometer equipped with a CuKa radiation source. In all instances, parallel beam optics with a flat graphite monochromator and a proportional counter were utilized. The diffractometer was calibrated with a silicon sample [58,59]. The residual stresses introduced by the shot peening process were measured throughout the thickness of the specimens using this XRD method. Residual stresses play a critical role in determining the material's structural integrity and long-term performance, especially in components subjected to cyclic loads, as they directly affect crack initiation and propagation. The residual stress profiles for the different shot-peened specimens are presented in Fig. 7.

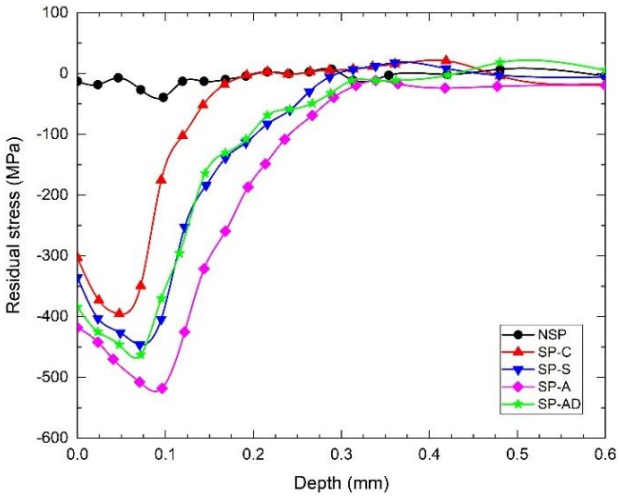

Fig. 7. Cross-sectional residual stress profiles of specimens.

These profiles provide a clear picture of how compressive residual stresses are distributed through the thickness of each specimen and highlight the effectiveness of the various shot peening treatments. Upon comparing the residual stress profiles for the different treatment conditions, it is evident that the maximum compressive residual stresses at the top surface vary across the specimens. Specifically, the maximum compressive residual stress values were found to be −395 MPa for the SP-C specimen, −446 MPa for SP-S, −517 MPa for SP-A, and −463 MPa for SP-AD. These variations indicate that the type and intensity of shot peening treatment have a significant impact on

the magnitude of residual stress induced at the surface. As expected, the highest compressive residual stresses were concentrated near the top surface of the material. The depth at which these stresses occur also varies among the specimens. For SP-C, the maximum compressive residual stress is achieved at a depth of 0.05 mm, while for SP-S and SP-A, this occurs at a depth of 0.075 mm. Interestingly, for the SP-AD specimen, the maximum compressive residual stress is located much closer to the surface, at a depth of only 0.1 mm. This distribution suggests that the shot peening process parameters, such as the intensity and pressure of the impacts, play a key role in how deeply the residual stresses penetrate into the material. As the depth increases, the intensity of residual stress gradually decreases. This reduction in stress with depth is a common observation in shot-peened materials and is attributed to the Bauschinger effect [60]. The Bauschinger effect occurs when the material undergoes plastic deformation in one direction (compression in this case), which reduces its ability to withstand subsequent deformation in the opposite direction. In other words, the further one moves from the shot-peened surface, the less pronounced the hardening effect becomes, and residual stresses eventually dissipate. In all specimens, no residual stress was detected at depths beyond 0.4 mm, indicating that the effects of shot peening are largely confined to the surface and near-surface regions of the material. Among the different shot peening treatments, the ascending severe shot peening treatment (ASSP) proved to be the most effective at inducing compressive residual stresses. The specimen treated with SP-A exhibited the highest maximum residual stress and maintained this stress at the greatest depth compared to other shot-peened samples. This correlates well with the microhardness measurements, where SP-A specimens also showed the greatest surface hardness and the deepest extent of hardening. The deeper penetration of residual stresses in SP-A-treated specimens suggests that this treatment not only enhances surface properties but also imparts greater resistance to fatigue and crack propagation over a larger volume of the material. Treatments like SP-A and SP-AD, which involve more sophisticated pressure application techniques, result in higher surface hardness and deeper stress penetration, offering superior mechanical performance compared to conventional shot peening processes.

3.4. Friction and wear behavior

The friction and wear behavior of the untreated (NSP) and shot-peened specimens (SP-C, SP-S, SP-A, and SP-AD) was assessed by conducting ball-on-disc tests to evaluate sliding wear resistance. This method is a widely accepted standard for investigating the tribological properties of materials, particularly in high-stress contact situations. The results of these tests are crucial for understanding how surface modifications, such as shot peening, influence the wear and frictional characteristics of treated materials. The wear volume of both untreated and treated specimens is shown in Fig. 8, and it is evident that the shot peening processes significantly reduce wear in comparison to the untreated surfaces. Shot peening treatments induce beneficial compressive residual stresses and enhance surface hardness, which together contribute to improved wear resistance. As Fig. 8 shows, the wear volume of SP-C, SP-A, and SP-AD was reduced by approximately 50%, compared with the non-treated samples.

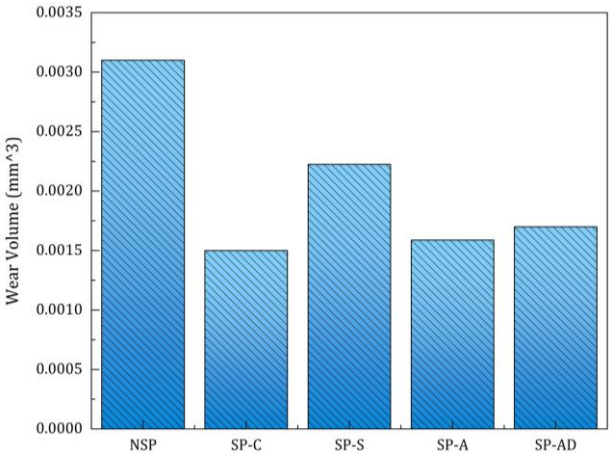

Fig. 8. Values of wear volume of all specimens.

For SP-A, the corresponding reduction was approximately 22%. Compared with the conventional shot-peening, the severe shot-peening did not make an improvement in wear resistance. This reduction in wear volume is a direct consequence of the enhanced surface hardness achieved through shot peening, as observed in Fig. 5, where the microhardness of treated specimens increased by a factor of two down to a depth of 0.1 mm. The Archard wear equation provides a theoretical basis for understanding this relationship. According to the equation, wear volume (V) is inversely proportional to the hardness (H) of the material, meaning that as

hardness increases, wear volume decreases. Since the shot peening treatments effectively doubled the surface hardness, it follows that the wear volume should be reduced to approximately half of what is observed in the untreated specimen. This correlation between surface hardness and wear resistance underscores the effectiveness of shot peening as a surface treatment process for improving the durability and longevity of materials exposed to sliding wear. In addition to wear volume, the frictional behavior of the specimens was also evaluated. The measured friction coefficients for NSP, SP-C, SP-S, SP-A, and SP-AD specimens are presented in Fig. 9.

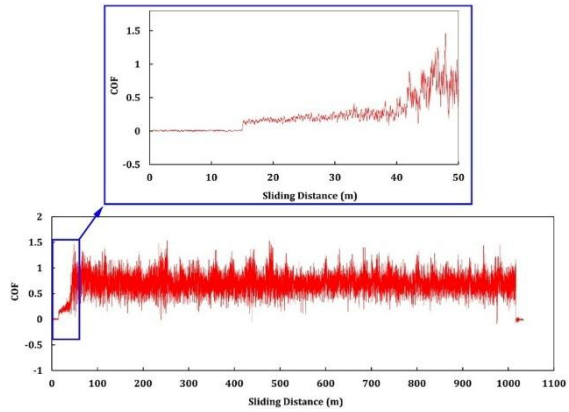

(a)

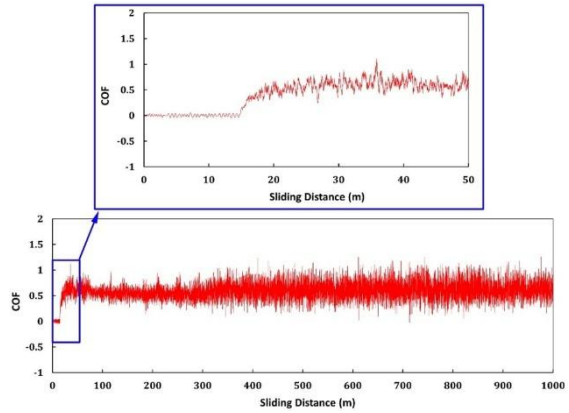

(b)

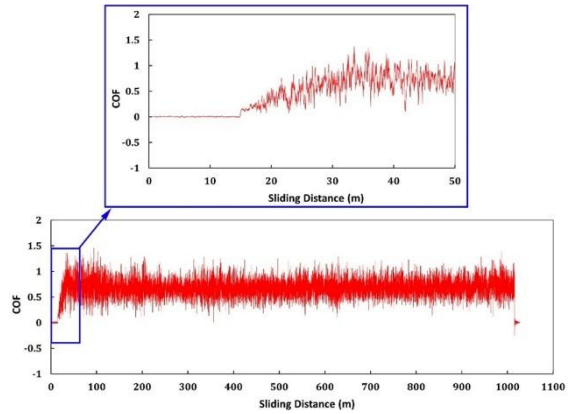

(c)

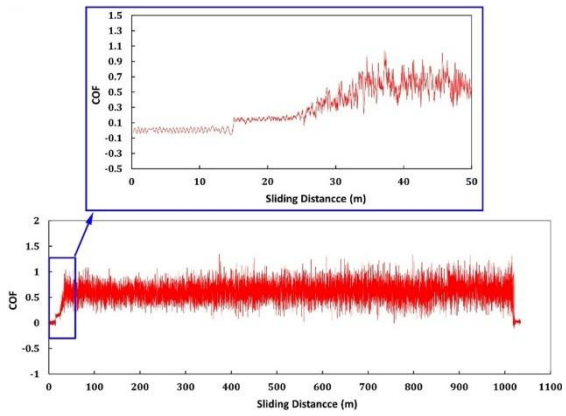

(d)

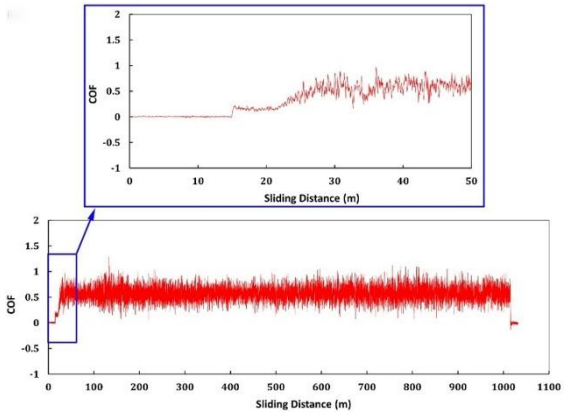

(e)

Fig. 9. Surface profiles across the wear tracks on the selected specimens; (a) NSP, (b) SP-C, (c) SP-S, (d) SP-A, and (e) SP-AD.

After an initial transitional period at the beginning of the test, where the friction coefficient fluctuates as the contact surfaces adjust, a steady-state friction coefficient was reached for each specimen. For the untreated (NSP) specimen, the steady-state friction coefficient was the highest at 0.75, indicating higher resistance to sliding and greater energy dissipation during contact. This higher friction coefficient suggests that the untreated surface experiences more severe frictional interactions, likely due to the absence of surface compressive residual stresses and the lower hardness. In contrast, the shot-peened specimens demonstrated lower steady-state friction coefficients, reflecting the benefits of the surface treatment. For SP-C, SP-S, SP-A, and SP-AD specimens, the steady-state friction coefficients were 0.65, 0.7, 0.6, and 0.6, respectively. The lower friction coefficients observed in the shot-peened specimens can be attributed to several factors. First, the increased surface hardness reduces the tendency of the surface to deform under contact, leading to a smoother sliding interface and, consequently, lower friction. Second, the

compressive residual stresses induced by the shot peening process help to mitigate the formation and propagation of surface cracks, further reducing friction. Among the treated specimens, the SP-A and SP-AD specimens exhibited the lowest friction coefficients, both stabilizing at 0.6. This result is consistent with the surface roughness measurements, which show that these specimens also had smoother surfaces compared to other shot-peened specimens. The smoother surface morphology, combined with the increased surface hardness, contributes to the reduced friction in these specimens, making them particularly well-suited for applications where both wear resistance and low friction are critical. In summary, the friction and wear behavior of the shot-peened specimens highlights the effectiveness of the treatment in enhancing both mechanical and tribological performance. By doubling the surface hardness and inducing compressive residual stresses, the shot peening process significantly reduces wear volume and lowers friction, offering a clear advantage over untreated materials.

Highest effects

Surface Layer Crystallization	Surface Roughness	Max Residual Stress	Hardening	Wear Volume
SP-A	SP-S	SP-A	SP-A	SP-C
SP-S	SP-A	SP-AD	SP-S	SP-A
SP-AD	SP-AD	SP-S	SP-AD	SP-AD
SP-C	SP-C	SP-C	SP-C	SP-S
NSP	NSP	NSP	NSP	NSP

Lowest effects

Fig. 10. Comparison of the obtained results.

The present study aims to compare various shot peening treatments, namely those with constant projection pressure (referred to as SP-C and SP-S) and treatments with gradient pressure (referred to as SP-A and SP-AD). The findings are summarized in Fig. 10, which illustrates the effectiveness of gradient severe shot peening treatments in improving mechanical and tribological properties. This type of visualization was presented by [61]. In this figure, all results are categorized based on their effects on various mechanical and metallurgical performance aspects. It is evident from the results that the SP-A treatment has the greatest impact on parameters such as surface layer crystallization size, maximum residual stress, and hardening. Conversely, the SP-S treatment exhibits significant effects on surface roughness, while the SP-C treatment shows minimal mass loss.

3.5. Surface morphology evaluation

To better understand the wear failure mechanism of as-received and shot peened specimens after the wear test, worn surfaces of the specimens were examined under the SEM as shown in Fig. 11. The examination showed significant characteristics indicative of adhesion wear mechanism, as well as the presence of debris, plastic deformation, and fatigue cracks in the worn surfaces of the specimens. The plastic deformation layer of wear scars was observed in SEM micrographs after the wear tests. The SEM micrographs displayed clear evidence of adhesion wear mechanism on the worn surfaces of the specimens. The formation of transfer films and material build-up was observed during sliding contact. The adhesion regions are observed in all specimens, especially NSP, SP-C, and SP-S. As can be seen, SP-S has the largest adhesion region among all specimens. Also, many debris particles were found dispersed across the worn surfaces, as seen in the SEM micrographs in all specimens. The particles are likely generated by the detachment of material from the surfaces due to repeated contact and relative motion. The presence of debris further supports the occurrence of abrasive wear mechanisms combined with adhesion wear. In addition, some plastic deformation marks were obvious in the SEM micrographs of the worn surfaces. Striations, grooves, and plastically deformed regions were observed, signifying the occurrence of severe mechanical interactions during sliding contact. Wear plastic deformation refers to the permanent deformation that occurs in materials during sliding contact and contributes to surface wear. During sliding, asperities on one surface interact with those on the opposing surface, leading to local stress concentrations. These stress concentrations cause the material to undergo plastic deformation in the form of microplasticity. Microplasticity refers to the overall deformation of a larger volume of material due to sliding contact. It involves more extensive plastic flow and can lead to the formation of wear scars or wear tracks on the material's surface. These wear scars often exhibit smooth and polished surfaces due to the cumulative effect of plastic deformation and material removal. Also, in the SP-S specimen, in addition to adhesion wear and plastic deformation, fatigue cracks were observed in the SEM micrographs. These cracks appeared as fine, branching lines on the worn surfaces.

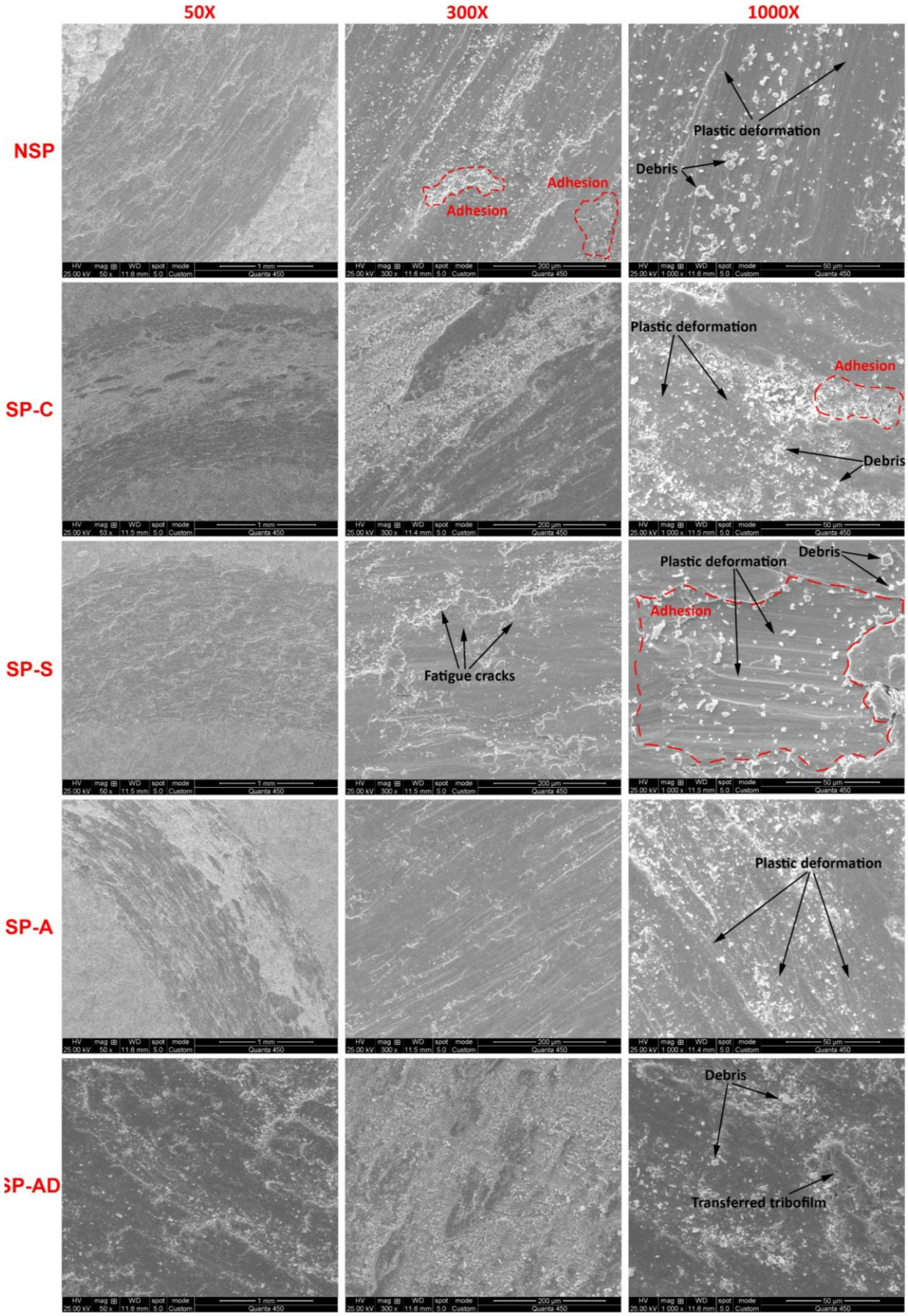

Fig. 11. SEM micrographs of worn surface of the specimens with different magnification (50X, 300X, and 1000X); (a), (b), (c) NSP, (d), (e), (f) SP-C, (g), (h), (i) SP-S, (j), (k), (l) SP-A, and (m), (n), (o) SP-AD.

The presence of fatigue cracks indicates the occurrence of fatigue wear. The presence of adhesion wear, debris particles, and plastic deformation further contributes to the generation and growth of these fatigue cracks. In the SP-AD specimen, some transferred tribo-films are observed. During sliding contact, asperities on the surface of one material come into contact with asperities on the opposing surface. As sliding continues, the junctions experience shear stresses, causing them to deform and eventually separate. This tearing phenomenon leads to the removal of material from one surface and its transfer to the other. The transferred material can form a thin layer or patches on the opposing surface, known as transfer films. These transfer films contribute to the further adhesion and subsequent wear process. The repetitive cycle of adhesion, deformation, and separation during sliding results in the formation of characteristic features such as wear debris, microcracks, and plastically deformed regions on the worn surfaces. Overall, the SEM analysis of the worn surfaces showed a complex wear behavior characterized by adhesion wear mechanism, debris accumulation, plastic deformation, and fatigue crack formation. Based on the SEM micrographs, it is evident that the NSP and SP-S specimens have exhibited a higher level of wear compared to the other specimens. This finding is consistent with the results obtained from the analysis of wear volume values.

4. CONCLUSION

In this work, we investigated the impact of the shot peening treatment method (GSSP) on AISI 304 steel, focusing on its microstructures, residual stress, mechanical properties, and tribological behavior. Experimental tests were conducted to analyze various aspects such as microstructure, grain size, surface topography, microhardness, and residual stresses. Optical microscopy and scanning electron microscopy were used to assess the microstructure of the shot-peened specimens. The mechanical properties were evaluated by measuring microhardness and roughness, while the XRD method was employed to measure the residual stress. The wear behavior was examined through a pin-on-disc test, and the worn surface topology was analyzed using scanning electron microscopy (SEM). Ultimately, a comparison was made between different shot-peened specimens based on the aforementioned measurements.

1. It can be observed that the depth of the plastically deformed layers is increased by increasing the kinetic energy of shot peeing. Also, grain refinement is achieved by increasing the severity of the shot peening treatment. It was observed that the microstructures of all specimens are formed by austenite grains inside which mechanical twining marks are observed.
2. The microhardness of samples treated with shot peening decreases as depth increases, with the highest value at the surface and the steady state value of approximately 202.5 HV at a depth of 0.4 mm and beyond. The lowest hardness value at the surface is that of SP-C at approximately 370 HV. The highest harness at the surface is that of SP-A at 410 HV.
3. The surface roughness measurements show that the gradient severe shot peening did not yield smoother surfaces than the conventional shot pinning treatment.
4. Residual stresses induced by the shot peening process along the thickness of the specimens were measured using the XRD method. Comparing the profiles of different specimens shows that the maximum compressive residual stress of the top surface was −395 MPa, −446 MPa, −517 MPa, and −463 MPa with the specimens of SP-C, SP-S, SP-A, and SP-AD, respectively. The maximum compressive residual stresses in shot-peened samples are achieved on the top near the surface and at depths of 0.05 mm, 0.075 mm, 0.075 mm, and 0.1 mm for SP-C, SP-S, SP-A, and SP-AD respectively.
5. The wear test results show surfaces treated with the SP-C, SP-A, and SP-AD experienced approximately ½ of the wear of the untreated surface while SP-S samples experienced ¾ of the wear of the untreated surface .
6. For the untreated specimen, the steady friction coefficient was the highest at 0.75. For SP-C, SP-S, SP-A, and SP-AD specimens, the steady friction coefficient was 0.65, 0.7, 0.6, and 0.6, respectively
7. A comparison of the obtained results shows the SP-A treatment has the greatest impact on parameters such as surface layer crystallization size, maximum residual stress, and hardening. Conversely, the SP-S treatment exhibits significant effects on surface roughness, while the SP-C treatment shows minimal mass loss.

8. SEM observation shows characteristics indicative of the adhesion wear mechanism, as well as the presence of debris, plastic deformation, and fatigue cracks in the worn surfaces of the specimens.
9. Further research is needed to optimize the tribological performance of GSSP-treated surfaces and understand the underlying wear mechanisms.

REFERENCES

[1] M. Kattoura, S. R. Mannava, D. Qian, and V. K. Vasudevan, "Effect of laser shock peening on residual stress, microstructure and fatigue behavior of ATI 718Plus alloy," *International Journal of Fatigue*, vol. 102, pp. 121–134, Apr. 2017, doi: 10.1016/j.ijfatigue.2017.04.016.

[2] E. Maleki, G. H. Farrahi, K. R. Kashyzadeh, O. Unal, M. Gugaliano, and S. Bagherifard, "Effects of conventional and severe shot peening on residual stress and fatigue Strength of steel AISI 1060 and residual stress relaxation due to fatigue loading: Experimental and numerical simulation," *Metals and Materials International*, vol. 27, no. 8, pp. 2575–2591, Oct. 2020, doi: 10.1007/s12540-020-00890-8.

[3] B. Salehnasab and E. Poursaeidi, "Mechanism and modeling of fatigue crack initiation and propagation in the directionally solidified CM186 LC blade of a gas turbine engine," *Engineering Fracture Mechanics*, vol. 225, p. 106842, Dec. 2019, doi: 10.1016/j.engfracmech.2019.106842.

[4] B. Salehnasab, D. Zarifpour, J. Marzbanrad, and G. Samimi, "An Investigation into the Fracture Behavior of the IN625 Hot-Rolled Superalloy," *Journal of Materials Engineering and Performance*, vol. 30, no. 10, pp. 7171–7184, May 2021, doi: 10.1007/s11665-021-05895-x.

[5] B. Salehnasab, E. Poursaeidi, S. A. Mortazavi, and G. H. Farokhian, "Hot corrosion failure in the first stage nozzle of a gas turbine engine," *Engineering Failure Analysis*, vol. 60, pp. 316–325, Dec. 2015, doi: 10.1016/j.engfailanal.2015.11.057.

[6] B. Salehnasab, J. Marzbanrad, and E. Poursaeidi, "Transient thermal fatigue crack propagation prediction in a gas turbine component," *Engineering Failure Analysis*, vol. 130, p. 105781, Sep. 2021, doi: 10.1016/j.engfailanal.2021.105781.

[7] K. H. S. Silva, J. R. Carneiro, R. S. Coelho, H. Pinto, and P. Brito, "Influence of shot peening on residual stresses and tribological behavior of cast and austempered ductile iron," *Wear*, vol. 440–441, p. 203099, Oct. 2019, doi: 10.1016/j.wear.2019.203099.

[8] H. Kovacı, İ. Hacısalihoğlu, A. F. Yetim, and A. Çelik, "Effects of shot peening pre-treatment and plasma nitriding parameters on the structural, mechanical and tribological properties of AISI 4140 low-alloy steel," *Surface and Coatings Technology*, vol. 358, pp. 256–265, Nov. 2018, doi: 10.1016/j.surfcoat.2018.11.043.

[9] B. Salehnasab, E. Hajjari, and S. A. Mortazavi, "Failure assessment of the first stage blade of a gas turbine engine," *Transactions of the Indian Institute of Metals*, vol. 70, no. 8, pp. 2103–2110, Jan. 2017, doi: 10.1007/s12666-016-1031-4.

[10] S. Pour-Ali, A.-R. Kiani-Rashid, and A. Babakhani, "Surface nanocrystallization and gradient microstructural evolutions in the surface layers of 321 stainless steel alloy treated via severe shot peening," *Vacuum*, vol. 144, pp. 152–159, Jul. 2017, doi: 10.1016/j.vacuum.2017.07.016.

[11] Y. Zhang, F. Lai, S. Qu, V. Ji, H. Liu, and X. Li, "Effect of shot peening on residual stress distribution and tribological behaviors of 17Cr2Ni2MoVNb steel," *Surface and Coatings Technology*, vol. 386, p. 125497, Feb. 2020, doi: 10.1016/j.surfcoat.2020.125497.

[12] R. F. Kubler, S. Berveiller, D. Bouscaud, R. Guiheux, E. Patoor, and Q. Puydt, "Shot peening of TRIP780 steel: Experimental analysis and numerical simulation," *Journal of Materials Processing Technology*, vol. 270, pp. 182–194, Feb. 2019, doi: 10.1016/j.jmatprotec.2019.02.031.

[13] G. H. Farrahi and H. Ghadbeigi, "An investigation into the effect of various surface treatments on fatigue life of a tool steel," *Journal of Materials Processing Technology*, vol. 174, no. 1–3, pp. 318–324, Mar. 2006, doi: 10.1016/j.jmatprotec.2006.01.014.

[14] O. Unal, E. Maleki, I. Kocabas, H. Yilmaz, and F. Husem, "Investigation of nanostructured surface layer of severe shot peened AISI 1045 steel via response surface methodology," *Measurement*, vol. 148, p. 106960, Aug. 2019, doi: 10.1016/j.measurement.2019.106960.

[15] S. Bagherifard, I. Fernandez-Pariente, R. Ghelichi, and M. Guagliano, "Effect of severe shot peening on microstructure and fatigue strength of cast iron," *International Journal of Fatigue*, vol. 65, pp. 64–70, Sep. 2013, doi: 10.1016/j.ijfatigue.2013.08.022.

[16] K. Lu and J. Lu, "Nanostructured surface layer on metallic materials induced by surface mechanical attrition treatment," *Materials Science and Engineering A*, vol. 375–377, pp. 38–45, Feb. 2004, doi: 10.1016/j.msea.2003.10.261.

[17] M. Multigner *et al.*, "Superficial severe plastic deformation of 316 LVM stainless steel through grit blasting: Effects on its microstructure and subsurface mechanical properties," *Surface and Coatings Technology*, vol. 205, no. 7, pp. 1830–1837, Sep. 2010, doi: 10.1016/j.surfcoat.2010.07.126.

[18] B. N. Mordyuk *et al.*, "Characterization of ultrasonically peened and laser-shock peened surface layers of AISI 321 stainless steel," *Surface and Coatings Technology*, vol. 202, no. 19, pp. 4875–4883, Apr. 2008, doi: 10.1016/j.surfcoat.2008.04.080.

[20] C. Brin, J. P. Rivière, J. P. Eymery, and J. P. Villain, "Structural characterization of wear debris produced during friction between two austenitic stainless steel antagonists," *Tribol. Lett.*, vol. 11, pp. 127–132, 2001, doi: 10.1023/A:1016612718139.

[21] M. R. Bateni, J. A. Szpunar, X. Wang, and D. Y. Li, "Wear and corrosion wear of medium carbon steel and 304 stainless steel," *Wear*, vol. 260, no. 1–2, pp. 116–122, Mar. 2005, doi: 10.1016/j.wear.2004.12.037.

[22] S. A. Khan, S. Shamail, S. Anwar, A. Hussain, S. Ahmad, and M. Saleh, "Wear performance of surface treated drills in high speed drilling of AISI 304 stainless steel," *Journal of Manufacturing Processes*, vol. 58, pp. 223–235, Aug. 2020, doi: 10.1016/j.jmapro.2020.08.022.

[23] Y. Sun, "Sliding wear behaviour of surface mechanical attrition treated AISI 304 stainless steel," *Tribology International*, vol. 57, pp. 67–75, Jul. 2012, doi: 10.1016/j.triboint.2012.07.015.

[24] M. Zandrahimi, M. R. Bateni, A. Poladi, and J. A. Szpunar, "The formation of martensite during wear of AISI 304 stainless steel," *Wear*, vol. 263, no. 1–6, pp. 674–678, May 2007, doi: 10.1016/j.wear.2007.01.107.

[25] A. Gariépy, H. Y. Miao, and M. Lévesque, "Simulation of the shot peening process with variable shot diameters and impacting velocities," *Advances in Engineering Software*, vol. 114, pp. 121–133, Jul. 2017, doi: 10.1016/j.advengsoft.2017.06.011.

[26] S. M. H. Gangaraj, M. Guagliano, and G. H. Farrahi, "An approach to relate shot peening finite element simulation to the actual coverage," *Surface and Coatings Technology*, vol. 243, pp. 39–45, Mar. 2012, doi: 10.1016/j.surfcoat.2012.03.057.

[27] J. Badreddine, E. Rouhaud, M. Micoulaut, and S. Remy, "Simulation of shot dynamics for ultrasonic shot peening: Effects of process parameters," *International Journal of Mechanical Sciences*, vol. 82, pp. 179–190, Mar. 2014, doi: 10.1016/j.ijmecsci.2014.03.006.

[28] B. Bhuvaraghan, S. M. Srinivasan, and B. Maffeo, "Numerical simulation of Almen strip response due to random impacts with strain-rate effects," *International Journal of Mechanical Sciences*, vol. 53, no. 6, pp. 417–424, Apr. 2011, doi: 10.1016/j.ijmecsci.2011.03.004.

[29] M. Guagliano, "Relating Almen intensity to residual stresses induced by shot peening: a numerical approach," *Journal of Materials Processing Technology*, vol. 110, no. 3, pp. 277–286, Apr. 2001, doi: 10.1016/s0924-0136(00)00893-1.

[30] G. H. Farrahi, J. L. Lebrijn, and D. Couratin, "Effect of shot peening on residual stress and fatigue life of a spring steel," *Fatigue & Fracture of Engineering Materials & Structures*, vol. 18, no. 2, pp. 211–220, Feb. 1995, doi: 10.1111/j.1460-2695.1995.tb00156.x.

[31] A. Ghasemi, S. M. Hassani-Gangaraj, A. H. Mahmoudi, G. H. Farrahi, and M. Guagliano, "Shot peening coverage effect on residual stress profile by FE random impact analysis," *Surface Engineering*, vol. 32, no. 11, pp. 861–870, Jul. 2016, doi: 10.1080/02670844.2016.1192336.

[32] E. Maleki and O. Unal, "Roles of surface coverage increase and re-peening on properties of AISI 1045 carbon steel in conventional and severe shot peening processes," *Surfaces and Interfaces*, vol. 11, pp. 82–90, Mar. 2018, doi: 10.1016/j.surfin.2018.03.003.

[33] O. Unal and R. Varol, "Almen intensity effect on microstructure and mechanical properties of low carbon steel subjected to severe shot peening," *Applied Surface Science*, vol. 290, pp. 40–47, Nov. 2013, doi: 10.1016/j.apsusc.2013.10.184.

[34] E. Maleki and O. Unal, "Shot peening process effects on metallurgical and mechanical properties of 316 l steel via: experimental and neural network modeling," *Metals and Materials International*, vol. 27, no. 2, pp. 262–276, Sep. 2019, doi: 10.1007/s12540-019-00448-3.

[35] A. H. Mahmoudi, A. Ghasemi, G. H. Farrahi, and K. Sherafatnia, "A comprehensive experimental and numerical study on redistribution of residual stresses by shot peening," *Materials & Design*, vol. 90, pp. 478–487, Nov. 2015, doi: 10.1016/j.matdes.2015.10.162.

[36] R. Karimbaev, Y.-S. Pyun, E. Maleki, O. Unal, and A. Amanov, "An improvement in fatigue behavior of AISI 4340 steel by shot peening and ultrasonic nanocrystal surface modification," *Materials Science and Engineering A*, vol. 791, p. 139752, Jun. 2020, doi: 10.1016/j.msea.2020.139752.

[37] A. Amanov, R. Karimbaev, E. Maleki, O. Unal, Y.-S. Pyun, and T. Amanov, "Effect of combined shot peening and ultrasonic nanocrystal surface

modification processes on the fatigue performance of AISI 304," *Surface and Coatings Technology*, vol. 358, pp. 695–705, Nov. 2018, doi: 10.1016/j.surfcoat.2018.11.100.

[38] N. E. Uzan, S. Ramati, R. Shneck, N. Frage, and O. Yeheskel, "On the effect of shot-peening on fatigue resistance of AlSi10Mg specimens fabricated by additive manufacturing using selective laser melting (AM-SLM)," *Additive Manufacturing*, vol. 21, pp. 458–464, Apr. 2018, doi: 10.1016/j.addma.2018.03.030.

[39] E. Maleki, O. Unal, and K. R. Kashyzadeh, "Fatigue behavior prediction and analysis of shot peened mild carbon steels," *International Journal of Fatigue*, vol. 116, pp. 48–67, Jun. 2018, doi: 10.1016/j.ijfatigue.2018.06.004.

[40] J. González, S. Bagherifard, M. Guagliano, and I. F. Pariente, "Influence of different shot peening treatments on surface state and fatigue behaviour of Al 6063 alloy," *Engineering Fracture Mechanics*, vol. 185, pp. 72–81, Mar. 2017, doi: 10.1016/j.engfracmech.2017.03.017.

[41] Q. Yang *et al.*, "Effect of different surface asperities and surface hardness induced by shot-peening on the fretting wear behavior of Ti-6Al-4V," *Surface and Coatings Technology*, vol. 349, pp. 1098–1106, Jul. 2018, doi: 10.1016/j.surfcoat.2018.06.092.

[42] Q. Yang *et al.*, "Investigation on the fretting fatigue behaviors of Ti-6Al-4V dovetail joint specimens treated with shot-peening," *Wear*, vol. 372–373, pp. 81–90, Dec. 2016, doi: 10.1016/j.wear.2016.12.004.

[43] K. Kubiak, S. Fouvry, A. M. Marechal, and J. M. Vernet, "Behaviour of shot peening combined with WC–Co HVOF coating under complex fretting wear and fretting fatigue loading conditions," *Surface and Coatings Technology*, vol. 201, no. 7, pp. 4323–4328, Sep. 2006, doi: 10.1016/j.surfcoat.2006.08.094.

[44] H. Kovacı, Y. B. Bozkurt, A. F. Yetim, M. Aslan, and A. Çelik, "The effect of surface plastic deformation produced by shot peening on corrosion behavior of a low-alloy steel," *Surface and Coatings Technology*, vol. 360, pp. 78–86, Jan. 2019, doi: 10.1016/j.surfcoat.2019.01.003.

[45] V. Pandey, J. K. Singh, K. Chattopadhyay, N. C. S. Srinivas, and V. Singh, "Influence of ultrasonic shot peening on corrosion behavior of 7075 aluminum alloy," *Journal of Alloys and Compounds*, vol. 723, pp. 826–840, Jun. 2017, doi: 10.1016/j.jallcom.2017.06.310.

[46] H. Kovacı, İ. Hacısalihoğlu, A. F. Yetim, and A. Çelik, "Effects of shot peening pre-treatment and plasma nitriding parameters on the structural, mechanical and tribological properties of AISI 4140 low-alloy steel," *Surface and Coatings Technology*, vol. 358, pp. 256–265, Nov. 2018, doi: 10.1016/j.surfcoat.2018.11.043.

[47] X. Wei, D. Zhu, W. Zhu, D. Wu, J. Li, and C. Zhang, "Effects of Surface Characteristics of AISI 304 Stainless Steel by Wet Shot Peening and its Wear and Corrosion Behavior," *International Journal of Electrochemical Science*, vol. 15, no. 6, pp. 4840–4852, May 2020, doi: 10.20964/2020.06.57.

[48] R. Gopi, I. Saravanan, A. Devaraju, and G. B. Loganathan, "Investigation of shot peening process on stainless steel and its effects for tribological applications," *Materials Today Proceedings*, vol. 22, pp. 580–584, Sep. 2019, doi: 10.1016/j.matpr.2019.08.215.

[49] Y. Y. Avcu, O. Yetik, M. Guney, E. Iakovakis, T. Sınmazçelik, and E. Avcu, "Surface, Subsurface and Tribological Properties of Ti6Al4V Alloy Shot Peened under Different Parameters," *Materials*, vol. 13, no. 19, p. 4363, Sep. 2020, doi: 10.3390/ma13194363.

[50] K. Zhan, Y. Zhang, S. Zhao, Z. Yang, B. Zhao, and V. Ji, "Tribological Behavior and Corrosion Resistance of S30432 Steel after Different Shot Peening Processes," *Journal of Materials Engineering and Performance*, vol. 31, no. 2, pp. 1250–1258, Sep. 2021, doi: 10.1007/s11665-021-06249-3.

[51] P. Q. Trung, N. W. Khun, and D. L. Butler, "Effects of shot peening pressure, media type and double shot peening on the microstructure, mechanical and tribological properties of low-alloy steel," *Surface Topography Metrology and Properties*, vol. 4, no. 4, p. 045001, Oct. 2016, doi: 10.1088/2051-672x/4/4/045001.

[52] E. Maleki, S. Bagherifard, O. Unal, M. Bandini, G. H. Farrahi, and M. Guagliano, "Introducing gradient severe shot peening as a novel mechanical surface treatment," *Scientific Reports*, vol. 11, no. 1, Nov. 2021, doi: 10.1038/s41598-021-01152-2.

[53] S. A. E. International, *AMS 2430S–2012: Shot Peening, Automatic*, SAE International, Warrendale, PA, USA, Jul. 2012.

[54] S. M. Hassani-Gangaraj, A. Moridi, M. Guagliano, A. Ghidini, and M. Boniardi, "The effect of nitriding, severe shot peening and their combination on the fatigue behavior and micro-structure of a low-alloy steel," *International Journal of Fatigue*, vol. 62, pp. 67–76, May 2013, doi: 10.1016/j.ijfatigue.2013.04.017.

[55] O. Unal, E. Maleki, I. Karademir, F. Husem, Y. Efe, and T. Das, "Effects of conventional shot peening, severe shot peening, re-shot peening and precised grinding operations on fatigue performance of AISI 1050 railway axle steel," *International Journal of Fatigue*, vol. 155, p. 106613, Oct. 2021, doi: 10.1016/j.ijfatigue.2021.106613.

[56] D. L. Dorset, "X-ray diffraction: a practical approach," *Microscopy and Microanalysis*, vol. 4, no. 5, pp. 513–515, Oct. 1998, doi: 10.1017/s143192769800049x.

[57] S. Sivasankaran, K. Sivaprasad, R. Narayanasamy, and P. V. Satyanarayana, "X-ray peak broadening analysis of AA 6061100–x–xwt.% Al2O3 nanocomposite prepared by mechanical alloying," *Materials Characterization*, vol. 62, no. 7, pp. 661–672, Apr. 2011, doi: 10.1016/j.matchar.2011.04.017.

[58] E. Atar, C. Sarioglu, U. Demirler, E. S. Kayali, and H. Cimenoglu, "Residual stress estimation of ceramic thin films by X-ray diffraction and indentation techniques," *Scripta Materialia*, vol. 48, no. 9, pp. 1331–1336, Mar. 2003, doi: 10.1016/s1359-6462(03)00019-8.

[59] C. Sarioglu, U. Demirler, M. K. Kazmanli, and M. Urgen, "Measurement of residual stresses by X-ray diffraction techniques in MoN and Mo2N coatings deposited by arc PVD on high-speed steel substrate," *Surface and Coatings Technology*, vol. 190, no. 2–3, pp. 238–243, Oct. 2004, doi: 10.1016/j.surfcoat.2004.08.184.

[60] S. Narita, K. Hayakawa, T. Uemori, and Y. Kubota, "Evaluation of strength of stainless steel bolt without heat treatment considering Bauschinger effect during manufacturing process," *Journal of Materials Processing Technology*, vol. 278, p. 116481, Nov. 2019, doi: 10.1016/j.jmatprotec.2019.116481.

[61] E. Maleki, O. Unal, M. Doubrava, L. Pantelejev, S. Bagherifard, and M. Guagliano, "Application of impact-based and laser-based severe plastic deformation methods on additively manufactured 316L: Microstructure, tensile and fatigue behaviors," *Materials Science and Engineering A*, vol. 916, p. 147360, Oct. 2024, doi: 10.1016/j.msea.2024.147360.